Available online at www.sciencedirect.com

ScienceDirect

Nuclear and Particle Physics Proceedings 273–275 (2016) 1185–1189

www.elsevier.com/locate/nppp

The tracker and calorimeter systems of the Mu2e experiment

David G. Hitlin[a]
for the Mu2e Collaboration

[a] *Lauritsen Laboratory, California Institute of Technology, Pasadena CA 91125 USA (hitlin@caltech.edu)*

Abstract

The Mu2e experiment at Fermilab is a sensitive search for lepton flavor violation via muon-to-electron conversion in the field of an aluminum nucleus. The requirements for the tracking and calorimeter systems of the experiment, as well as the design of systems that fulfill these requirements, are briefly described.

1. Introduction

The Mu2e experiment at Fermilab is designed to search for the charged lepton flavor-violating process of the conversion of a negative muon into an electron in the field of an aluminium nucleus. The expected single event sensitivity of the experiment is 6 x 10^{-17}, an improvement of four orders of magnitude over the current best limit [1][2]. We will describe herein two of the detector systems of the experiment, the straw tube tracker and the crystal calorimeter, that are .used to identify the conversion electron signal, an electron whose momentum is the mass of a muon less the binding energy of the Al muonic atom, approximately 104 MeV/*c*, and to control backgrounds in the signal region which are required to be less than 0.2 events at the experiment's design sensitivity.

2. The Mu2e detector

The Mu2e apparatus is shown in Figure 1. The experiment consists of are three large solenoids: a Production Solenoid (PS) having a graded field from 2.5 to 4.6T) in which a pulsed proton beam from the redesigned Fermilab accelerator complex produces pions in a tungsten target, followed by an S-shaped Transport Solenoid (TS) with fields varying between 2.5 and 2T, that views the target in the backward direction for background rejection, and forms a negative muon beam with a spectrum peaking around 40 MeV/*c* that enters a large Detector Solenoid (DS) having a field of 2T upstream, tapering to a uniform 1T in the tracker/calorimeter region. The solenoids are surrounded by a large Cosmic Ray Veto system (not shown). The aluminium muon stopping target, tracker and calorimeter are aligned along the axis of the 1T solenoidal magnetic field of the DS, having a gradient in the stopping target region and a constant field downstream of the target. The conversion electron trajectory is thus a helix whose radius initially increases and is then approximately constant in the tracker and calorimeter region. The tracker and the calorimeter each are designed to have sensitive regions that approximate an annulus in order to allow the very substantial rates from lower momentum background processes at smaller helical radii to pass through them unimpeded.

This paper will describe the requirements for the tracker and calorimeter systems of the Mu2e experiment, as well as their realization in the chosen technologies.

http://dx.doi.org/10.1016/j.nuclphysbps.2015.09.186

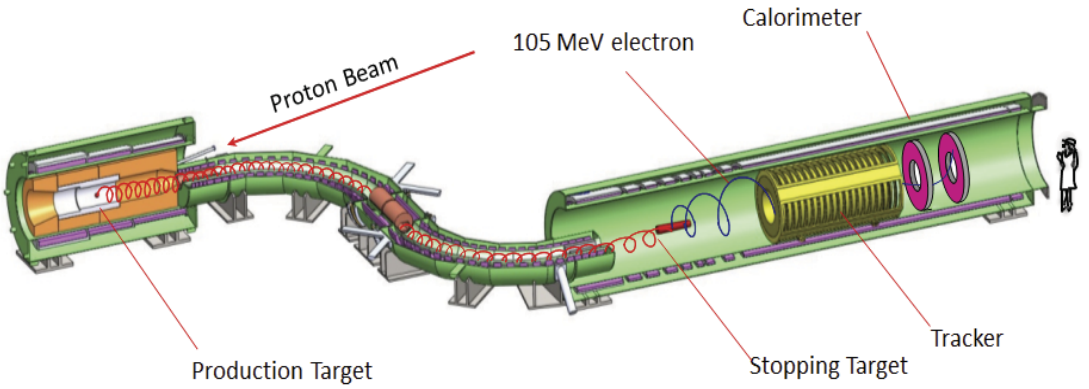

Figure 1. The components of the Mu2e experiment. From the left: the Production Solenoid and target, the S-shaped Transport Solenoid and collimator and the Detector Solenoid, containing the muon stopping target, the straw tube tracking chamber and the crystal calorimeter disks. The cosmic ray veto system is not shown.

3. Tracker requirements

The active area of the tracker extends from about $40 < r < 70$ cm (where the radius r is measured from the solenoid axis), providing good acceptance for signal electrons while not intercepting most electrons produced by muons that decay in orbit in the Al muonic atom (DIO electrons) (including electrons scattered into the acceptance), These dimensions have been optimized to maximize the acceptance to conversion electrons while minimizing the number of low energy electrons that intersect the tracker. Mechanical support, readout electronics, *etc*. are placed at $r > 70$ cm, outside the acceptance for signal and DIO electrons.

The momentum resolution requirement is based on background rejection: the signal is sharply peaked, whereas backgrounds are broad (cosmic rays, radiative pion capture) or steeply falling (DIO electrons) (see Figure 1). For width of the (asymmetric, non-gaussian) error distribution must be $\sigma < 180$ keV/c. Scattering and straggling in material upstream of the tracker are significant contributors to the resolution.

The detectors are in vacuum in order to minimize scattering through the measurement region and dE/dx straggling throughout the entire path for signal electrons, as well as to reduce scattering of DIO electrons into the tracker. This also eliminates muon stops from the remnant muon beam with residual gas.

The tracker will be designed for an overall mean time to failure (MTTF) of >1 year. If they can be kept isolated, a few dead channels will not constitute a tracker failure requiring access. The ability to isolate local failures is an important part of the design. In particular, the capability to remotely disconnect high voltage to each straw will be implemented so that a few broken or otherwise defective wires will not necessitate an access.

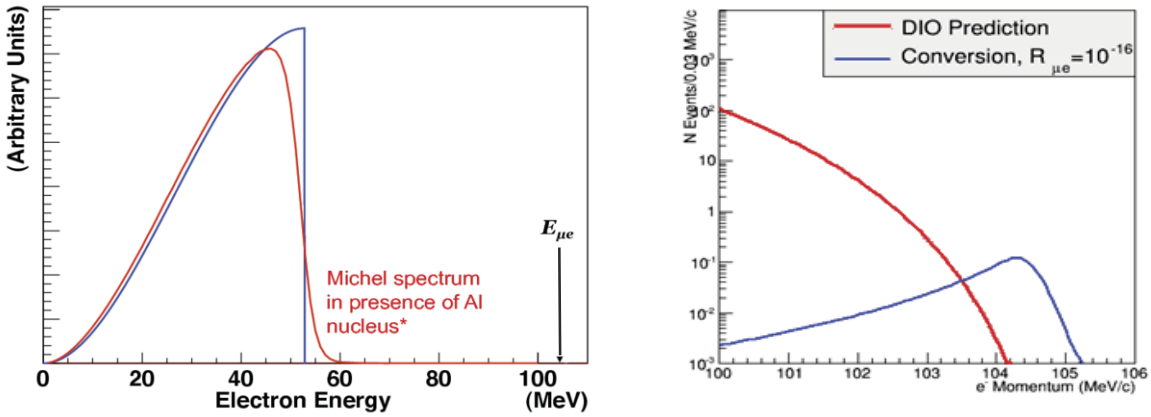

Figure 2. Left. The electron spectrum from free muon decay (blue), the spectrum of muons decaying from orbit in a muonic aluminum atom (red) and the nearly mono-energetic spectrum of conversion electrons (black). Right. The signal region. The conversion electron spectrum for a rate of 10^{-16} is shown in blue, the tail of the DIO spectrum in red.

The tracker must also tolerate a "beam flash" prior to the live window, and be efficient at the peak rates at the start of the live window. Actual rates depend on detector geometry and are presented later.

During the live window, half of the hits in the detector are from slow protons ($\lesssim$100 MeV/c momentum or ~5 MeV kinetic energy) ejected from the stopping target. The tracker must have sufficient dE/dx resolution to distinguish these protons from electrons.

4. Tracker design

Three 120° panels complete the ring of one face; another three panels, rotated by 30°, complete another ring on the opposing face. After the plane is assembled. This arrangement has been found to give the best stereo performance. A pair of identical planes form a ***station***. During assembly the 2nd plane is rotated 180° around a vertical axis.

Eighteen stations are assembled into the completed tracker, shown in Figure 4. Horizontal beams maintain longitudinal alignment of the rings. The thicker ring seen at the upstream end, and the two thinner rings placed between stations at the downstream end, stiffen the structure. Stiffening rings and beams are stainless steel.

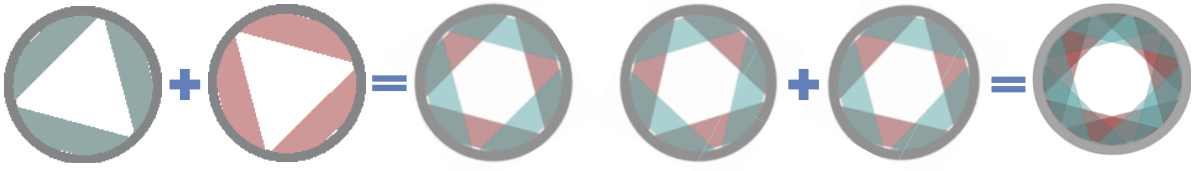

Figure 3. Assembly of a tracker station. Six panels of 96 groups of straws are assembled into a panel. Two panels form a tracker station.

The selected design for the Mu2e tracker is a low mass array of drift tubes aligned transverse to the DS axis. The basic detector element is a 25 µm sense wire inside a 5 mm diameter "straw tube". Each straw consists of two layers of ~6 µm (25 gauge) Mylar®, spiral wound, with a ~3 µm layer of adhesive between layers, for a total wall thickness of 15 µm. The inner cathode surface has 500 Å of aluminum overlaid with 200 Å of gold. A 500 Å aluminum coating on the outer surface serves as additional electrostatic shielding to and reduce the leak rate.

The active length of straws varies from 334 mm to 1174 mm. The straws, supported only at their ends, are kept straight under an initial tension of 700 g. Mylar® is sensitive to humidity and creeps (gradually stretches) under stress. Both creep and hygroscopic expansion of Mylar® are less than that of the more widely used Kapton® straws. Nonetheless, the straw tension will decrease to ~400g over the lifetime of the experiment due to stress relaxation.

The assembly of straws into panels and stations is shown in Figure 3. Groups of 96 straws are assembled into ***panels***. Each panel covers a 120° arc with two layers of straws. The double layer improves efficiency and helps resolve the "left-right" ambiguity. A 1.25 mm gap between straws allows for manufacturing tolerances and expansion due to gas pressure. Individual straws must therefore be self-supporting across their span.

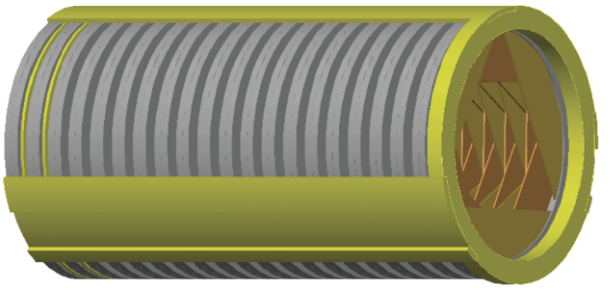

Figure 4. The tracker system consists of eighteen stations.

The momentum resolution performance of the tracker is shown in Figure 5.

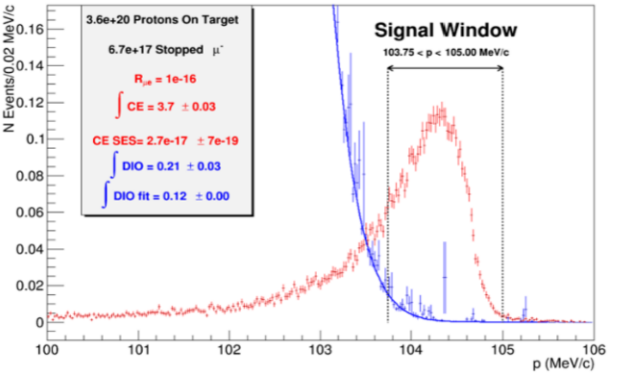

Figure 5. Momentum resolution for conversion electrons and DIO background, with a signal-to-noise ratio corresponding to Rμe of 10^{-16}.

5. Calorimeter requirements

The primary functions of the calorimeter are to provide energy, position and timing information to confirm that events reconstructed by the tracker are well measured and are not the result of a spurious combination of hits. Moreover, the calorimeter should also provide the experiment's trigger. This leads to the following requirements:

- An energy resolution of 5% at 100 MeV is desirable to confirm the electron momentum measurement from the tracker, which is much more precise.
- A time resolution better than ~ 0.5 ns is required to ensure that energy deposits in the
- calorimeter are in time with events reconstructed in the tracker.
- A position resolution better than 1 cm is necessary to allow comparison of the position of the energy deposit to the extrapolated trajectory of a reconstructed track.
- The calorimeter should provide additional information that can be combined with information from the tracker to distinguish muons from electrons.
- The calorimeter must provide a trigger, either in hardware or software, that can be used to identify events with significant energy deposits.
-
- The calorimeter must operate in the unique, high-rate Mu2e environment and must maintain functionality for radiation exposures up to 20 Gy/crystal/year and for a neutron flux equivalent to 10^{11} $n_{\_1MeV\ eq}$ /cm^2.

The energy resolution of a crystal calorimeter complements, but is not competitive with, that of the tracking detector. Provided that there is excellent time resolution, even a relatively coarse confirmation of track energy by the calorimeter will, however, help reject backgrounds from spurious combinations of hits from lower energy beam particles and cosmic ray muons that evade the Cosmic Ray Veto system.

6. Calorimeter design

In the 100 MeV energy regime, a total absorption calorimeter employing a homogeneous continuous medium is required to meet the energy resolution

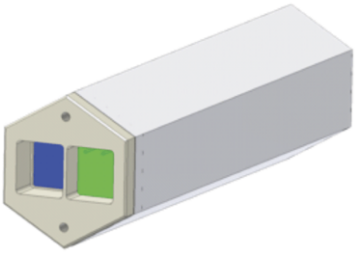

Figure 6. A hexagonal BaF2 crystal read out by two independent avalanche photodiodes.

requirement; we have chosen a crystal-based design. Two types of crystals have been considered in detail for the calorimeter: lutetium-yttrium oxyorthosilicate (LYSO) and barium fluoride (BaF_2). Due to the large and increasing cost of LYSO, the baseline design selected for the Mu2e calorimeter is an array of BaF_2 crystals arranged in two annular disks. Electrons following helical trajectories spiral into the front faces of the crystals, as shown in Figure 5. Photo-detectors, electronics and services are mounted on the rear face of the disks. The crystals are of hexagonal shape, 33 mm across flats and are 200 mm (~$10X_0$) long; there are a total of ~1650 crystals, each read out by two large-area APDs; solid-state photo-detectors are required because the calorimeter resides in a 1 T magnetic field. Front-end electronics is mounted on the rear of each disk, while voltage distribution, slow controls and digitizer electronics are mounted behind each disk. A laser flasher system provides light to each crystal for relative calibration and monitoring purposes. A circulating liquid radioactive source system provides absolute calibration and an energy scale. The crystals are supported by a stainless steel support structure, shown in Figure 7

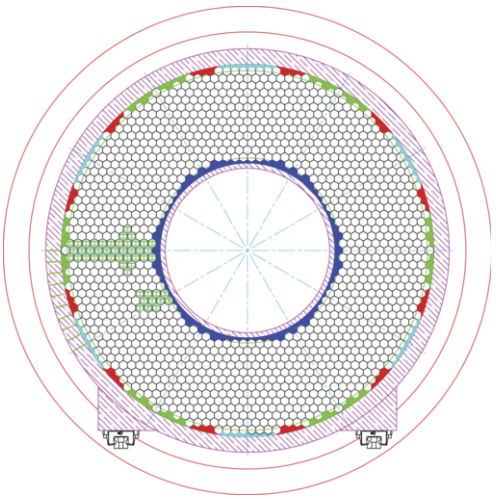

Figure 7. Arrangement of the hexagonal crystals in the annular support structure. There are two such identical disks.

Barium fluoride has a fast scintillation component (decay time 900 ps) at 220 nm and a much larger slow component (decay time 630 ns) at 300 nm. The spectrum is shown in Figure 8. In order to take advantage of the time resolution and background rejection capabilities afforded by the fast component, need a photosensor that has high quantum efficiency at 220 nm and strong rejection of the 300 nm component. An avalanche photodiode with the required characteristics is currently under development by a Caltech/JPL/RMDinc consortium. The calculated quantum efficiency as a function of wavelength for three, five and seven layer filters, constructed by atomic layer deposition is also shown in Figure 8. The quantum efficiency and timing characteristics of the device are also improved over conventional APDs by improving the internal distribution of electric field using a super-lattice constructed using molecular beam epitaxy.

A detailed simulation of thee energy response of the BaF_2 calorimeter is shown in Figure 9; the resolution (FWHM/2.35) from a fit of a two-sided Crystal Ball function, is 4.3% for 105 MeV/*c* conversion electrons. Equally important, the time resolution is estimated to be substantially better than the 500 ps requirement needed to separate electrons produced by cosmic ray muons in the detector from conversion electrons (see Figure 10). The discrimination requires both timing information from the calorimeter and *dE/dx* information from the tracker.

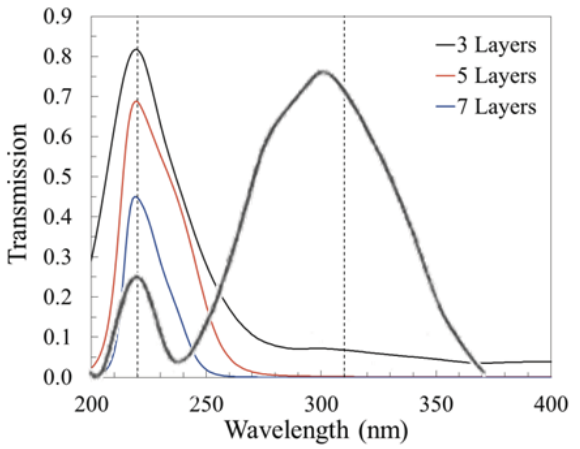

Figure 8. Scintillation spectrum of BaF_2, showing fast (0.9) ns decay component at 220 nm and the slow (630 ns) component at 300 nm. The response of the superlattice APD currently under development is shown for 3, 5 and 7 layer integrated filters.

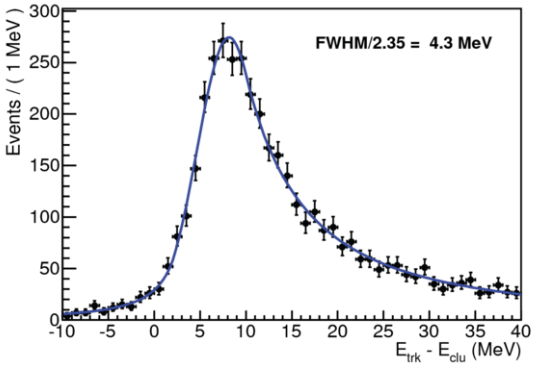

Figure 9. Calculated energy resolution of the calorimeter, fitted with a pair of Crystal Ball functions, yielding a FWHM/2.35 = 4.3MeV for conversion electrons.

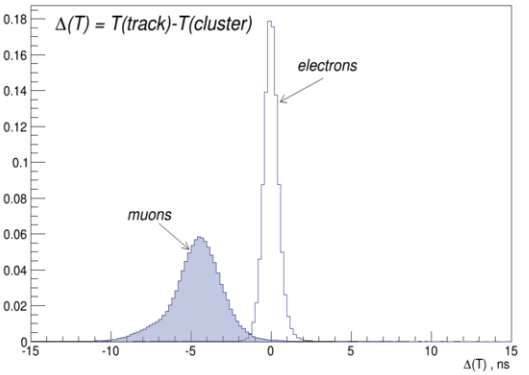

Figure 10. Difference between tracker and calorimeter determination of track time for electrons and muons calculated assuming an electron hypothesis.

7. Conclusion

The design of the tracker and calorimeter systems of the Mu2e experiment appears to fulfil the stringent requirements posed by a search for the rare m to e conversion process with a sensitivity improvement of four orders of magnitude beyond present limits.

References

[1] Mu2e Conceptual Design Report, R.J. Abrams *et al.,* arXiv:1211.7019 [physics.ins-det].
[2] Mu2e Technical Design Report, L. Bartoszek, *et al.,* arXiv:1501.05241v2 [physics.ins-det].